

# STUDY OF A SOLAR ENERGY KALINA CYCLE APPLIED IN BOM JESUS DA LAPA - BAHIA

G. S. Amorim<sup>a</sup> ABSTRACT

A. I. Sato<sup>b</sup>

A. B. Souza<sup>c</sup>

<sup>a,b,c</sup> Universidade Federal do Oeste da Bahia,  
Centro Multidisciplinar de Bom Jesus da Lapa,  
CEP 47600-000, Bom Jesus da Lapa, Bahia,  
Brasil.

<sup>a</sup> gessica.amorim@ufob.edu.br

<sup>b</sup> andre.sato@ufob.edu.br

<sup>c</sup> anderson.souza@ufob.edu.br

V. M. Rodrigues<sup>d</sup>

<sup>d</sup> Universidade Federal do Oeste do Pará, Instituto  
de Engenharia e Geociências. CEP 68035-110,  
Santarém, Pará, Brasil.

<sup>d</sup> vicente.ufopa@gmail.com

Received: Sept 20, 2022

Revised: Sept 23, 2022

Accepted: Sept 30, 2022

Modern population's needs increased demands for electricity in such a way that new energy sources were explored, in search of lower environment impacts and fossil fuels dependency. Renewable energy sources for electricity production, such as solar and wind energy, have significantly attracted attention and places as the west region of Bahia state has a good potential for its application. This location is characterized by high solar irradiance of 2136 kWh/m<sup>2</sup> a year, already having 4 photovoltaic power plants in operation and 2 more in project phases. Another possible application is the solar thermal energy and Kalina Cycle presents as a good possibility for employing it, since the non-azeotropic mixture of ammonia-water as working fluid allows low temperature heat sources utilization. Based on that, this research proposed the study of a Kalina power cycle, with steady state conditions, using thermal solar energy as low temperature heat source and applied to the solar irradiance of Bom Jesus da Lapa – BA. The thermodynamic cycle was developed and simulated with Engineering Equation Solver (EES®), thermal efficiency was analyzed by varying parameters such as: heat source temperature from 90 °C to 120 °C, high pressure line from 10 to 35 bar and ammonia mass fraction from 0.35 to 0.95. The final cycle presented a superheater before the turbine and a regenerator with poor ammonia-water mixture from the separator (as hot side) and ammonia-water mixture before entering the boiler (as cold side). Results indicated maximum efficiency of ~7.4%, with high pressure side of 35 bar, heat source temperature of 120 °C, superheater heat source temperature of 200 °C and ammonia mass fraction of 0.64 kg/kg.

**Keywords:** Kalina power cycle, thermodynamic cycle, thermal solar energy

## INTRODUCTION

In the last years, research on energy conversion with low temperature sources have gained attention specially by the usage of renewable energy sources such as: biomass, geothermal and solar thermal energy. In this vast front, this work intends to focus on a relatively new power cycle called Kalina Cycle and its application at Bom Jesus da Lapa – BA conditions (solar radiance and ambient temperature).

The Kalina Cycle was first introduced by Kalina (1983), using a non-azeotropic mixture of ammonia-water as working fluid and comparing it with a conventional Rankine Cycle at a cogeneration application. Results indicated that the Kalina Cycle had higher efficiency by using higher fluid pressure and because the fluid mixture had variable boiling temperature.

Different approaches has been studied since then, Srinivas *et al.* (2019) presented three configurations for the Kalina Cycle based on applied source temperature: high (400-600°C), medium (~300°C) and low (100-

200°C) temperatures. Also analyzing the usage of cogeneration and several construction options.

For low temperature sources, Sun *et al.* (2014) and Hettiarachchi *et al.* (2007) applied a Kalina Cycle to solar energy and geothermal energy, respectively. By evaluating the influence of several variables on the cycle efficiency, the authors indicated that mass fraction and mass flow of the ammonia-water mixture and inlet pressure at the turbine had the major contributions on this analysis. Besides that, it was possible to conclude that the maximum thermodynamic efficiency could be achieved with a specific operation condition of mass fraction and turbine inlet pressure.

Although Rankine Cycle can also be used with low temperature sources, Shokati *et al.* (2015) applied exergoeconomic concepts to compare four different power cycles using geothermal energy source (Variable Pressure, Conventional and Double Fluid Organic Rankine Cycles, and Kalina Cycle). Results presented that Kalina Cycle had lower work output but higher

exergoeconomic efficiency with the lowest unitary energy price.

In this concept, the application of Kalina Cycle with thermal solar energy is of great prospect, especially for the west region of Bahia state, presenting a mean solar irradiance of 2136 kWh/m<sup>2</sup> throughout the year (Atlas Solar Bahia, 2018). This paper objective is to study the application of a Kalina Cycle, based on low temperature heat source, for usage with solar thermal apparatus in Bom Jesus da Lapa – BA climatic conditions. Results presented the comparison of a simple power cycle and with regeneration and superheater.

## KALINA CYCLE

A basic Kalina Cycle was analyzed based on Srinivas *et al.* (2019) work, and presented in Figure 1. Superheated steam expands in the turbine (1), converting fluid energy into mechanical energy. Saturated steam (2) is then mixed with the saturated liquid ammonia-water mixture (8) that exits the separator. The mixture of phases, rich steam phase mixture and poor liquid phase mixture (3) proceeds to the absorber, in which ammonia is absorbed while the steam phase is condensed (4) and pumped into the boiler (5). The boiler heats the fluid to a temperature between the dew point and the bubble point of the mixture and then sends it to the separator (6). Wet steam is divided into saturated steam rich in ammonia (1) and saturated liquid low in ammonia (7), due to the difference in density between the fluids.

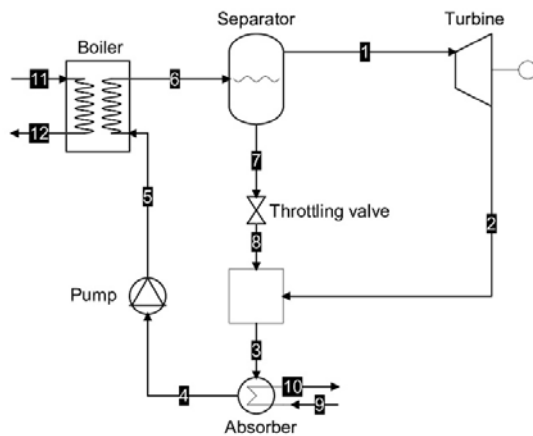


Figure 1. Basic Kalina Cycle. Source: modified from Srinivas *et al.* (2019).

An alternative cycle with solar thermal energy usage can be seen in (WANG *et al.*, 2013). Authors presented the possibility to use a storage system, preventing temperature fluctuations inside the boiler, as presented in Figure 2. A secondary cycle is responsible to accommodate the solar collectors array and, using a thermal fluid such as molten salt or oil, storage the energy inside thermal storage tanks that can be used throughout the day. There is also a possibility of a secondary heater

setup that can work with periods of insufficient solar radiation.

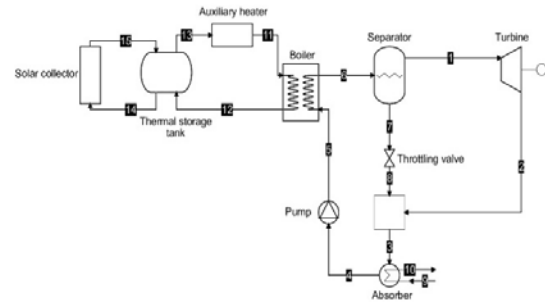


Figure 2. Solar energy driven Kalina Cycle. Source: modified from Wang *et al.* (2013).

## Thermodynamic properties of ammonia-water mixture

Using a multi-component fluid as a working fluid, specifically a non-azeotropic mixture, allows the cycle to operate at varying boiling and condensing temperatures. Thus, the work flexibility of these binary steam power cycles to operate at different temperatures in heat exchangers is greater than the cycles that usually use only pure fluids (MORAN *et al.*, 2018).

Another advantage associated with these fluids is the lower irreversibility from heat transfer in the boiler and condenser, increasing the total efficiency of the cycle (SECKIN, 2018). This fact is associated with the temperature behavior between the saturation points of the non-azeotropic mixture (bubble point and dew point), as illustrated in the diagram in Figure 3.

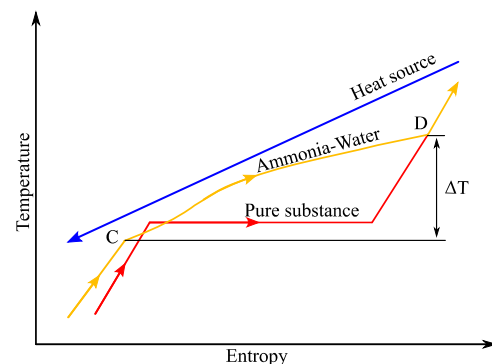


Figure 3 – Non-azeotropic mixture (ammonia-water) and pure substance heat exchange. Source: Author (2021).

For the thermodynamic properties evaluation of the mixture, many studies on the thermodynamic properties of the ammonia-water mixture and pressure ranges for power cycle to refrigeration applications (Ibrahim; Klein, 1993; Shankar Ganesh; Srinivas, 2011; Thorin, 2001; Thorin; Dejfors; Svedberg, 1998; Xu; Goswami, 1999; Ziegler; Trepp, 1984).

In this study, equations of state for the mixture were based on the model presented by Ibrahim and Klein (1993) and already implemented in EES® software.

### METHODOLOGY

Initially, the thermodynamic model was based on a basic Kalina cycle operating with a unitary mass flow of the working fluid at points (4) to (6) and as shown in Figure 1. In it, the equipment consisted in absorber, condenser, pump, evaporator, separator, turbine, expansion valve and mixing tank. Additionally, climatic radiation data was collected of Bom Jesus da Lapa – BA – from the National Institute of Meteorology (INMET) – to determine the mean solar irradiance and ambient temperature for a period of last 10 years, between (2009 – 2019).

The thermodynamic modeling was performed according to some flow design assumptions:

- Operation in steady state regime.
- Negligible pressure losses.
- Isobaric process, except for turbine, pump, and expansion device.
- Expansion valve works as an isenthalpic device.
- Negligible heat losses.
- Separator outflow: saturated liquid (7) and saturated steam (1).

Therminol VP-1 oil was selected as the hot side heat transfer fluid, since, according to Qu *et al.* (2017) and Ashouri *et al.* (2015), it is commonly used in this type of application. The specific heat of Therminol VP-1 oil was specified using Eq. (1) (Ashouri *et al.*, 2015), with T as the temperature and  $(C_p)_{oil}$  as the specific heat.

$$(C_p)_{oil} = \frac{0.002414T}{2} + 5.9591 \times 10^{-6} \times \left(\frac{T}{2}\right)^2 - 2.9879 \times 10^{-8} \times \left(\frac{T}{2}\right)^3 + 4.4172 \times 10^{-11} \times \left(\frac{T}{2}\right)^4 + 1.498 \quad (1)$$

Also, a superheater before the turbine and a regenerator positioned at the separator outlet/evaporator inlet were added to the cycle for comparison purposes, the construction is indicated in Figure 4. Inlet temperature in the superheater was considered equal to 200°C to prevent fluid condensation inside the turbine. Still, the bulk of the heating fluid flow was at 120°C, which is an easily achievable temperature with solar heating systems and at the studied city climate conditions.

Subsequently, conservation of mass and energy – corresponding to Eq. (2) and (3) – were applied to each device in the cycle. With  $\dot{m}_i$  representing the mass flow at the inlet,  $\dot{m}_o$  the mass flow at the outlet,  $h$  as the ammonia-water enthalpy,  $\dot{Q}$  the heat transfer rate and  $\dot{W}$  the power output.

$$\sum_i \dot{m}_i - \sum_s \dot{m}_o = 0 \quad (2)$$

$$\dot{Q} - \dot{W} + \sum_i \dot{m}_i h_i - \sum_o \dot{m}_o h_o = 0 \quad (3)$$

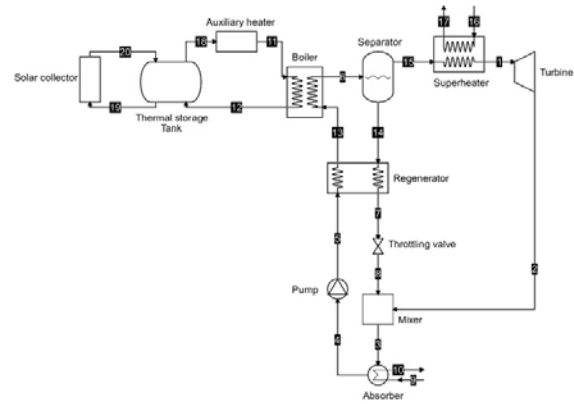


Figure 4. Kalina Cycle with Regenerator and Superheater. Source: modified from Srinivas; Shankar; Ganesh (2019).

For the absorber, energy and mass equations can be expressed as Eq. (4) and (5). With  $Q_a$  representing the heat dissipated to the cooling water,  $(C_p)_w$  the specific heat of the water,  $T$  as the temperatures,  $\dot{m}$  the mass flow, and  $h$  as the ammonia-water enthalpy.

$$\dot{m}_3 = \dot{m}_4 \quad (4)$$

$$Q_a = \dot{m}_9(T_{10} - T_9)(C_p)_w = \dot{m}_3(h_3 - h_4) \quad (5)$$

For the pump, energy and mass equations can be expressed as Eq. (6) and (7). With  $\dot{W}_p$  representing the power required at the pump.

$$\dot{m}_4 = \dot{m}_5 \quad (6)$$

$$\dot{W}_p = \dot{m}_4(h_5 - h_4) \quad (7)$$

For the boiler, energy and mass equations can be expressed as Eq. (8) and (9). With  $\dot{Q}_b$  representing the heat transfer rate in the boiler, and  $(C_p)_{oil}$  the specific heat of the oil.

$$\dot{m}_{13} = \dot{m}_6 \quad (8)$$

$$\dot{Q}_b = \dot{m}_{11}(T_{11} - T_{12})(C_p)_{oil} = \dot{m}_6(h_6 - h_{13}) \quad (9)$$

For the separator, energy and mass equations can be expressed as Eq. (10) and (11).

$$\dot{m}_6 = \dot{m}_{14} + \dot{m}_{15} \quad (10)$$

$$\dot{m}_6 h_6 = \dot{m}_{14} h_{14} + \dot{m}_{15} h_{15} \quad (11)$$

For the turbine, energy and mass equations can be expressed as Eq. (12) and (13). With  $\dot{W}_t$  representing the power output of the turbine.

$$\dot{m}_1 = \dot{m}_2 \quad (12)$$

$$\dot{W}_t = \dot{m}_1 (h_1 - h_2) \quad (13)$$

For the mixer, energy and mass equations can be expressed as Eq. (14) and (15).

$$\dot{m}_3 = \dot{m}_2 + \dot{m}_8 \quad (14)$$

$$\dot{m}_3 h_3 = \dot{m}_2 h_2 + \dot{m}_8 h_8 \quad (15)$$

For the superheat, energy and mass equations can be expressed as Eq. (16) and (17). With  $\dot{Q}_s$  representing the heat transfer rate in the superheat.

$$\dot{m}_1 = \dot{m}_{15} \quad (16)$$

$$\begin{aligned} \dot{Q}_s &= \dot{m}_{16} (T_{16} - T_{17}) (C_p)_{oil} \\ &= \dot{m}_{15} (h_1 - h_{15}) \end{aligned} \quad (17)$$

For the regenerator, energy and mass equations can be expressed as Eq. (18) and (19). With  $\dot{Q}_r$  representing the heat transfer rate in the regenerator.

$$\dot{m}_5 = \dot{m}_{13} \text{ e } \dot{m}_7 = \dot{m}_{14} \quad (18)$$

$$\dot{Q}_r = \dot{m}_5 (h_{13} - h_5) = \dot{m}_{14} (h_{14} - h_7) \quad (19)$$

The boiler outlet mixture temperature ( $T_6$ ) was determined based on the inlet temperatures of the heating fluid ( $T_{11}$ ) and a preestablished pinch point (PP). In this case, the method described by Kim *et al.* (2014) was used to determine undefined temperatures from the boiler, considering that the PP of a binary mixture is not located at the inlet/outlet of the heat exchangers or at the saturated liquid step as in pure substances.

Then, the ammonia mass fraction ( $x_6$ ) and turbine inlet pressure equal to  $P_6$  were varied to find optimal operating pair, which would present higher thermal efficiency for the cycle. The ranges in which these properties were analyzed can be seen in Table 1.

Through a preliminary evaluation, the radiation value found for an average day from data collected between 2009-2019 was equivalent to 489.9 W/m<sup>2</sup>, along

a period of 11 hour of sunlight and at Bom Jesus da Lapa – BA.

Table 1. Analyzed parameters. Source: author (2021).

Properties	Range
Pressure after Boiler ( $P_6$ )	10.00 to 35.00 bar
Ammonia mass fraction ( $x_{13}$ )	0.3500 to 0.9500 kg/kg

Through a preliminary evaluation, the radiation value found for an average day from data collected between 2009-2019 was equivalent to 489.9 W/m<sup>2</sup>, along a period of 11 hour of sunlight and at Bom Jesus da Lapa – BA. As for the ambient temperature, a maximum value below 34 °C was achieved during the average day (INMET, 2018). Based on the previous parameters, adopted values for pressure and temperature were established as presented in Table 2, also the turbine efficiency  $\eta_t$  and pump efficiency  $\eta_p$  were established.

Table 2. Adopted values for pressure, temperature, and efficiency. Source: authors (2021).

Input variable	Value	Unit
$T_9$	40.00	°C
$T_{10}$	50.00	°C
$T_{11}$	120.0	°C
$T_{16}$	200.0	°C
PP	10.00	°C
$\eta_t$	80.00	%
$\eta_p$	65.00	%

Considering a solar energy system with thermal storage as presented before, the temperature at points (11) and (16) is considered constant. Different thermal storages can be used for both the fluid temperatures or a single storage with thermal stratification. Since the basis of this study focuses on thermal Kalina Cycle, a simplified analysis of the thermal storage is presented by sizing the thermal storage volume for the boiler with Eq. (20). With  $V_b$  as the thermal storage volume,  $\rho_{oil}$  as the specific mass of the oil and  $t$  as the time interval for the thermal storage operation.

$$V_b = \frac{Q_b}{(C_p)_{oil} \rho_{oil} (T_{11} - T_{12})} t \quad (20)$$

The thermal storage volume for the superheater is expressed by Eq. (21). With  $V_s$  as the thermal storage volume for the superheater oil.

$$V_s = \frac{Q_s}{(C_p)_{oil} \rho_{oil} (T_{16} - T_{17})} t \quad (21)$$

The solar collectors evaluation from studies of Wang *et al.* (2013) and Ashouri *et al.* (2015), considered CPC (Compound Parabolic Collector) and PTC (Parabolic Trough Collector) as the most viable options for this application, because of their capability of achieving higher temperature, compared to flat-plate collectors.

**RESULTS**

Expected behavior of efficiency as a function of pressure and ammonia mass fraction for the basic cycle and the superheater/regenerator cycle are presented in Figure 5 (a) and (b), respectively, indicating an increasing thermodynamic efficiency for higher pressure and mass fraction values, with a maximum condition at which efficiency would decrease.

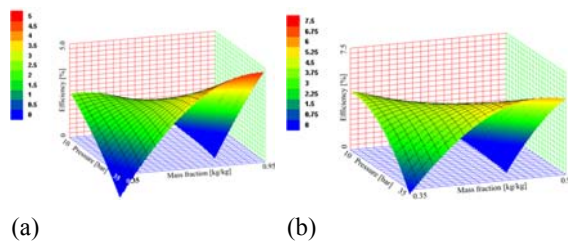


Figure 5. Thermal efficiency as function of ammonia mass fraction and pressure, for: (a) basic cycle and (b) superheater/regenerator cycle. Source: authors (2021).

For better visualization, thermal efficiencies for the basic cycle presented in Figure 1, as a function of inlet turbine pressure and mass fraction of the mixture after boiler are indicated in Figure 6 and Figure 7. The behavior presented indicates a maximum efficiency for a pair with optimum values of approximately 35.00 bar and 0.7800 kg/kg. Simulations with  $x_6$  above 0.7800 kg/kg resulted in lower values and were discarded.

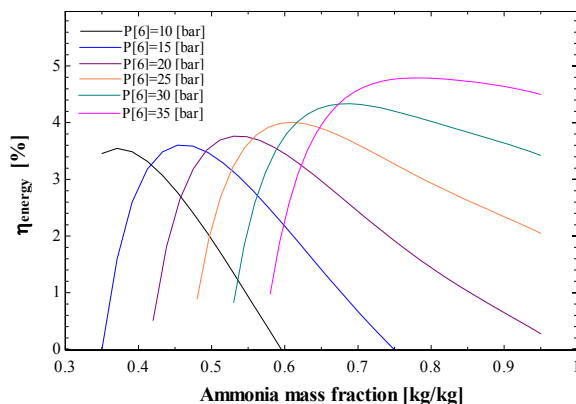


Figure 6. Basic cycle thermal efficiency vs. ammonia mass fraction, for 6 turbine inlet pressures. Source: authors (2021).

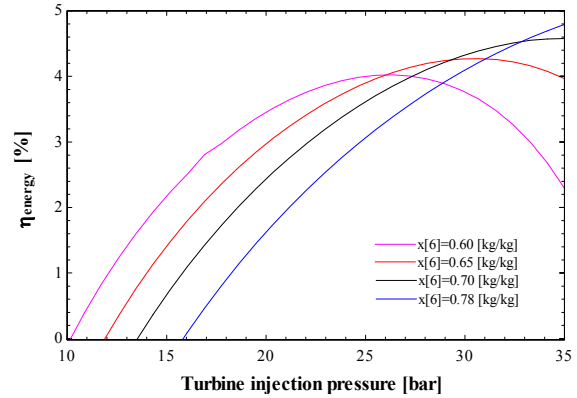


Figure 7. Basic cycle thermal efficiency vs. turbine inlet pressure for 4 ammonia mass fractions. Source: authors (2021).

For the cycle with regenerator and superheater, thermodynamic efficiency as a function of  $x_6$  was evaluated for 6 different values of  $P_6$  and are presented in Figure 8. Increases in turbine inlet pressure made the Kalina cycle more efficient and, for a given pressure, there was an ideal ammonia fraction whose efficiency reached its maximum value, and then decreased as the ammonia concentration was increased, same behavior can be seen in Hettiarachchi *et al.* (2007). Considering the maximum pressure curve equal to 35 bar, it is noticed that the ideal ammonia concentration is located at the equivalent point between 0.60 – 0.65 kg/kg.

Considering the interval for ammonia mass fraction between 0.62 to 0.65, the influence of turbine inlet pressure was analyzed for 4 different values and plotted in Figure 9. It is possible to observe that the curve for 0.62 kg/kg presents an upward behavior until reaches a maximum value at pressure equals to 34 bar. Similar behavior is expected to other 3 curves but, since limited to 35 bar, the curves of 0.64 kg/kg and 0.65 kg/kg will reach their optimum point at a pressure equal to or greater than the analyzed limit pressure. In this case, the curve corresponding to 0.64 kg/kg is responsible for generating greater efficiency for the pressure range analyzed.

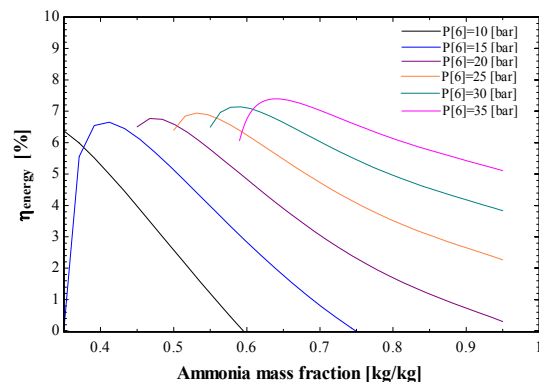


Figure 8. Regenerator/superheater cycle thermal efficiency vs. ammonia mass fraction, for 6 turbine inlet pressures. Source: authors (2021).

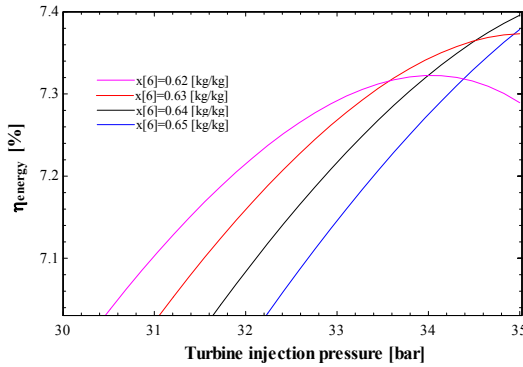


Figure 9. Regenerator/superheater cycle thermal efficiency vs. turbine inlet pressure for 4 ammonia mass fractions. Source: authors (2021).

Table 3 shows the maximum efficiency for all mass fraction curves, also presenting the associated pressure for the previous cycle. The last three concentrations analyzed achieved greater efficiency for a pressure of 35 bar, which did not allow us to identify whether it is the global maximum point of each curve. Differently, the curve of 0.62 kg/kg reached a maximum value for a pressure lower than 35 bar, but generated a lower efficiency than the others, making its use unfeasible. Therefore, it is possible to determine that the cycle will become more efficient working at a maximum pressure of 35 bar and an intermediate mass flow of ammonia of 0.64 kg/kg.

Table 3. Mass fraction and Pressure pair for thermal efficiency analysis. Source: authors (2021).

$x_6$ (kg/kg)	$\eta$ (%)	$P_6$ (bar)
0.6200	7.323	34.04
0.6300	7.373	35.00
0.6400	7.396	35.00
0.6500	7.379	35.00

With similar considerations for the basic cycle, the efficiency of the adopted settings can be seen in Table 4. As presented, the basic cycle produced an output of  $\dot{W}_t = 37.70 \text{ kW}$  while the superheater plus regenerator produced  $\dot{W}_t = 22.73 \text{ kW}$ . It is important to note that, although the second cycle had a lower output compared to the first one, the heat transfer rate at the heat source was considerably lower and, thus, increasing the thermodynamic efficiency. Also, the pre-established values of pressure and temperature contributed to these results.

Considering a daily operation of this final cycle, with a boiler consuming 265.6 kW of thermal energy, through 24 hours, a thermal reservoir of the selected oil would have a capacity of approximately 353 m<sup>3</sup> for the application and at 120°C – according to Eq. (20). While the superheater, would consume 41.82 kW, in need of a

reservoir of approximately 26 m<sup>3</sup> reservoir for the fluid at 200°C – according to Eq. (21).

Table 4. Thermal efficiency for the considered Kalina cycles. Source: author (2021).

Cycle	$x_6$ (kg/kg)	$P_6$ (bar)	$\dot{Q}_s$ (kW)	$\dot{W}_t$ (kW)	$\eta$ (%)
Basic	0.7800	35.00	786.9	37.70	4.791
Regenerator + Superheater	0.6400	35.00	307.4	22.73	7.396

Considering a regenerator located at the separator outlet/evaporator inlet followed by a superheater before the turbine, the system had significant increase in the thermodynamic performance of the Kalina cycle. Higher pressure at the turbine inlet would result in higher efficiency but, for the purpose of this study, 35 bar was established as an up limit. The properties' values of each state of the cycle, as shown in Figure 2, can be seen in Table 5. For  $q$  representing the quality of the working fluid at the analyzed points. It can be noticed that only ~17% of the fluid mass flow is directed to the turbine, with the rest of it returning to the mixer tank at a high temperature and suitable to the regenerator application.

Table 5. Thermodynamic values of the Kalina cycle. Source: authors (2021).

Point	$P$ (bar)	$T$ (°C)	$h$ (kJ/kg)	$x$ (kg/kg)	$q$	$\dot{m}$ (kg/s)
1	35.00	190.0	1685	0.9817	S.V <sup>(1)</sup>	0.1713
2	11.55	106.8	1519	0.9817	S.V <sup>(1)</sup>	0.1713
3	11.55	60.75	296.8	0.6400	0.1907	1.000
4	11.55	50.00	12.97	0.6400	S.L <sup>(1)</sup>	1.000
5	35.00	50.73	17.83	0.6400	C.L <sup>(1)</sup>	1.000
6	35.00	110.0	481.2	0.6400	0.1713	1.000
7	35.00	60.73	44.10	0.5694	C.L <sup>(1)</sup>	0.8287
8	11.55	59.29	44.10	0.5694	0.006449	0.8287
9	-	40.00	-	-	-	6.782
10	-	50.00	-	-	-	6.782
11	-	120.0	-	-	-	11.60
12	-	106.2	-	-	-	11.60
13	35.00	91.77	215.6	0.6400	C.L <sup>(1)</sup>	1.000
14	35.00	110.0	282.8	0.5694	S.L <sup>(1)</sup>	0.8287
15	35.00	110.0	1441	0.9817	Sa.V <sup>(1)</sup>	0.1713
16	-	200.0	-	-	-	0.3152
17	-	120.0	-	-	-	0.3152

<sup>(1)</sup> C.L is compressed liquid, S.V is superheated vapor, S.L is saturated liquid, and Sa.V is saturated vapor.

The solar system for each thermal fluid temperature used could be achieved with 2 different heating cycles, using PTC or CPC strategies. Further studies would be applied to analyze the necessary area of solar collector and the possibility for PVC integration.

## CONCLUSION

The Kalina cycle was thermodynamically analyzed for the application of low temperature source, considering thermal solar energy, and associated with a thermal

storage. The application of regenerator and superheater was essential to improve the efficiency of the cycle when compared to the basic cycle, presenting an increase of approximately 2.6% in the thermodynamic efficiency. The thermodynamic analysis results indicated that the greater the turbine inlet pressure, the greater the cycle efficiency. Furthermore, for a given pressure there was an ammonia concentration that generated the maximum efficiency; in this case, for 35.00 bar at  $P_6$  and 0.6400 kg/kg at  $x_{13}$ , the Kalina cycle presented  $\eta \approx 7.4\%$ , with a power output of  $\dot{W}_t = 22.73$  kW and for a mixture mass flow of  $\dot{m}_6 = 1$  kg/s. A 353 m<sup>3</sup> thermal reservoir and another of 26 m<sup>3</sup> should provide thermal oil, respectively, at 120.0 °C and 200.0 °C throughout a daily operation of the presented cycle and considering the application of CPC or PTC.

### ACKNOWLEDGEMENTS

The authors would like to thank the Universidade Federal do Oeste da Bahia (UFOB) and the Conselho Nacional de Desenvolvimento Científico e Tecnológico (CNPq) for their support.

### REFERENCE

- Ashouri, M., Vandani, A. M. K., And Mehrpooya, M., 2015. "Techno-economic assessment of a Kalina cycle driven by a parabolic Trough solar collector". *Energy Conversion and Management*, v. 105, pp. 1328–1339.
- Atlas Solar: Bahia, 2018. Curitiba: Camargo Schubert. Salvador: Secti: Seinfra: Cimatec/Senai, Pp.76.
- Hettiarachchi, H. D.M., Golubovic, M., Worek, W. M., And Ikegami, Y., 2007. "The performance of the Kalina cycle system 11(kcs-11) with low-temperature heat sources". *Journal of Energy Resources Technology*, Transactions of the ASME, [s. l.], v. 129, n. 3, pp. 243–247.
- Ibrahim, O. M., And Klein, S. A., 1993. "Thermodynamic Properties of Ammonia-Water Mixtures". *ASHRAE Transactions: Symposia*, v. 21, n. 2, pp. 1495.
- INMET, 2020, *Instituto Nacional de Metrologia*. <https://bdmep.inmet.gov.br/>. Accessed 09 October 2020.
- Kalina, A. I., 1983. "Combined Cycle and Waste Heat Recovery Power Systems Based on a Novel Thermodynamic Energy Cycle Utilizing Low-Temperature Heat for Power Generation". *ASME The American Society of Mechanical Engineers*, v. 83-JPGC-GT-3.
- Kim, K. H., Ko, H. J., And Kim, K., 2014. "Assessment of pinch point characteristics in heat exchangers and condensers of ammonia-water based power cycles". *Applied Energy*, v. 113, pp. 970–981.
- Qu, W., Su, B., Tang, S., And Hong, H., 2017. "Thermodynamic Evaluation of a hybrid solar concentrating photovoltaic/Kalina cycle for full spectrum utilization". *Energy Procedia*, v. 142, pp. 597–602.
- Shokati, N., Ranjbar, F., And Yari, M., 2015. "Exergoeconomic analysis and optimization of basic , dual-pressure and dual- fluid ORCs and Kalina geothermal power plants : A comparative study." *Renewable Energy*, v. 83, pp. 527–542.
- Srinivas, T., Shankar, R., And Ganesh, N. S., 2019. *Flexible Kalina Cycle Systems*. Apple Academic Press (AAP), Canada.
- Sun, F., Zhou, W., Ikegami, Y., Nakagami, K., and SU, X, 2014. "Energy-Exergy Analysis and Optimization of the Solar-Boosted Kalina Cycle System 11 (KCS-11)". *Renewable Energy*, v. 66, pp. 268–279.
- Ziegler, B., And Trepp, C, 1984. "Equation of state for ammonia-water mixtures". *International Journal of Refrigeration*, , v. 7, n. 2, pp. 101–106.

### RESPONSIBILITY NOTICE

The authors are the only responsible for the printed material included in this paper.